

# Effects of Cooking on the Cell Walls (Dietary Fiber) of ‘Scarlet Warren’ Winter Squash (*Cucurbita maxima*) Studied by Polysaccharide Linkage Analysis and Solid-State $^{13}\text{C}$ NMR

R. M. Sunil Ratnayake,<sup>†</sup> Ian M. Sims,<sup>§</sup> Roger H. Newman,<sup>§,⊥</sup> and Laurence D. Melton<sup>\*,†</sup>

<sup>†</sup>Food Science, Department of Chemistry, University of Auckland, Private Bag 92 019, Auckland, New Zealand

<sup>§</sup>Industrial Research Limited, P.O. Box 31 310, Lower Hutt, Wellington, New Zealand

**ABSTRACT:** Cell wall polysaccharides of ‘Scarlet Warren’ winter squash (*Cucurbita maxima*) were investigated before and after thermal processing. Linkage analysis of polysaccharides was done by gas chromatography coupled to mass spectrometry (GC-MS). The linkage analysis showed the cell wall polysaccharide compositions of raw and cooked squash were similar. The total pectic polysaccharides (galacturonan, rhamnogalacturonan, arabinan, and arabinogalactan) contents of the cell walls of both raw and cooked squash were 39 mol %. The amounts of pectic polysaccharides and xyloglucan in the cell walls of squash showed little alteration on heating. The cellulose content of the raw and cooked cell walls was relatively high at 47 mol %, whereas the xyloglucan content was low at 4 mol %. Solid-state  $^{13}\text{C}$  nuclear magnetic resonance (NMR) spectroscopy techniques were used to examine the molecular motion of the polysaccharides in the cell walls. The mobility of highly flexible galactan depends on the water content of the sample, but no difference was seen between raw and cooked samples. Likewise, the mobility of semimobile pectic polysaccharides was apparently unaltered by cooking. No change was detected in the rigid cellulose microfibrils on cooking.

**KEYWORDS:** *Cucurbita maxima*, winter squash, ‘Scarlet Warren’, thermal processing, cellulose crystallites, cell wall polysaccharides, solid-state  $^{13}\text{C}$  NMR, cross-polarization magic angle spinning (CP/MAS), single-pulse excitation magic angle spinning (SPE/MAS), proton spin relaxation editing (PSRE)

## INTRODUCTION

Plant cell walls serve a number of functions. They are organelles, which form a protective layer around each cell. By adhering to adjacent cell walls and by countering the turgor pressure, primary cell walls give the plant tissue its mechanical strength and, consequently, directly influence the texture of fruit and vegetables. As organelles they play an essential role in the life of plant cells.<sup>1</sup> They are biochemically active and are systematically modified<sup>2</sup> and replaced (turned over).<sup>3</sup>

The three-dimensional structure of primary cell walls has not been fully elucidated, but considerable progress has been made over the past decade. Cellulose has been shown to exist as individual microfibrils<sup>4</sup> in ordered layers.<sup>5–8</sup> The hemicelluloses, xyloglucan, xylans, and mannan, adhere to the cellulose microfibrils and serve to keep the microfibrils apart and are postulated to act as cross-links between the cellulose microfibrils to form a three-dimensional network. However, the earlier suggestion that cellulose microfibrils are coated with xyloglucan has not been observed, nor is it necessary for the functioning of the walls.<sup>8–11</sup> In an exciting development, the pectin side chains, galactan and arabinan, have also been found to adhere to cellulose microfibrils and so connect the flexible pectin gel network with the xyloglucan–cellulose assembly.<sup>12,13</sup> A third minor glycoprotein network exists in cell walls.<sup>14</sup> In an alternative model of the primary cell wall the cellulose microfibrils are surrounded by a layer of pectins and hemicelluloses that becomes less dense as the distance from the microfibril surface increases and there are no cross-links joining one microfibril to another.<sup>15,16</sup>

The texture of raw vegetables is expected to be altered by processing. Yet, until recently, little work was done to study the

changes in cell wall composition on processing. Changes in the cell wall components during cooking have now been investigated in a number of vegetables, including potato,<sup>17,18</sup> carrots,<sup>19</sup> buttercup squash,<sup>20</sup> and taro.<sup>21</sup> Heat-induced softening of vegetables is attributed largely to the depolymerization, solubilization, and losses of pectic polysaccharides from cell walls.<sup>17,19</sup>

The investigation of ‘Scarlet Warren’ squash, also known as ‘Red Warren’ pumpkin (*Cucurbita maxima*), was part of a larger study to understand and improve the quality of winter squash.<sup>20,22–24</sup> For the larger study ‘Scarlet Warren’, an orange, warty-skinned, low-starch, moist, and fibrous open-pollinated squash variety, was crossed with ‘CF2’ and ‘CF4’, two starchy inbred buttercup squash lines,<sup>24</sup> to obtain an improved buttercup squash cultivar, which is a major vegetable export for New Zealand. There has been additional research on pectin extracted from buttercup squash<sup>25</sup> and pumpkin.<sup>26,27</sup>

Solid-state  $^{13}\text{C}$  nuclear magnetic resonance (NMR) spectroscopy can be used to acquire details on molecular structures as well as information about the spatial arrangement and mobility of polysaccharides in plant cell walls.<sup>28–31</sup> Moreover, the changes in each cell wall component polysaccharides caused by thermal processing may be monitored by solid-state  $^{13}\text{C}$  NMR spectroscopy. Solid-state  $^{13}\text{C}$  NMR has been used to probe plant cell walls in different ways. The technique of cross-polarization magic angle spinning

**Received:** December 13, 2010

**Revised:** May 17, 2011

**Accepted:** May 23, 2011

**Published:** May 24, 2011

**Table 1. Glycosyl Linkage Composition of Cell Walls and Second HEPES-Soluble Fraction of Raw and Cooked ‘Scarlet Warren’ Squash at 2 Months of Storage<sup>a</sup>**

monosaccharide	deduced linkage	raw cell walls (mol %)	cooked cell walls (mol %)	raw second HEPES (mol %)	cooked second HEPES (mol %)
Araf	terminal	0.7	0.8	1.6	nd
	5-	1.0	1.4	1.2	nd
Xylp	terminal	0.6	0.6	nd	nd
	2-	0.3	0.4	nd	nd
	4-	1.0	1.3	nd	nd
	2,4-	tr	tr	nd	nd
Fucp	terminal	0.3	0.1	nd	nd
Rhap	2-	0.9	1.3	1.4	nd
	2,4-	0.8	1.0	0.6	nd
Manp	4-	3.1	3.5	tr	nd
	2,4-	0.3	0.4	tr	nd
	3,4,6-	tr	tr	nd	nd
GlcP	terminal	0.4	0.5	tr	9.0
	4-	48.1	47.0	12.6	78.3
	2,4-	0.5	0.4	nd	nd
	3,4-	0.6	0.6	nd	nd
	4,6-	2.0	1.9	tr	3.2
	2,4,6-	0.1	nd	nd	nd
	3,4,6-	0.2	0.2	nd	nd
Galp	terminal	1.4	1.7	1.6	nd
	4-	11.3	9.9	15.5	1.9
	3,4-	0.5	0.6	tr	nd
	4,6-	0.6	0.7	0.4	nd
	3,6-	nd	nd	nd	nd
	3,4,6-	tr	tr	nd	nd
GalApOMe	4-	17.2 (71.1)	18.6 (75.9)	42.2 (62.5)	4.3 (57.3)
GalAp	4-	7.0	5.9	25.3	3.2

<sup>a</sup> Determined by GC-MS and expressed as mol %. Data represent the mean of three analyses. Numbers in parentheses are degree of esterification. tr, trace (< 0.1 mol %); nd, not detected; 5-Araf, 5-linked arabinofuranose; t-Fucp, terminal fucopyranose; 2-Rhap, 2-linked rhamnopyranose; 2-Xylp, 2-linked xylopyranose; 4-GlcP, 4-linked glucopyranose; 4-Galp, 4-linked galactopyranose; 4-GalApOMe, methyl-esterified 4-linked galacturonic acid; 4-Galp, 4-linked galacturonic acid.

(CP/MAS) <sup>13</sup>C NMR has been used to examine the molecular ordering of cellulose in primary cell walls.<sup>32–35</sup> Single-pulse excitation (SPE) <sup>13</sup>C NMR spectroscopy has been used to investigate the composition of the highly mobile polysaccharides in cell walls.<sup>29,34</sup> In addition, proton spin relaxation editing (PSRE) <sup>13</sup>C NMR spectroscopy can be used to study the mobility of noncellulosic polysaccharides in cell walls of various fruits and vegetables including apple,<sup>28</sup> celery,<sup>9</sup> strawberry,<sup>36</sup> onion,<sup>34,37,38</sup> pineapple,<sup>38</sup> and cabbage.<sup>38</sup>

In the current project carbohydrate linkage analysis was used to determine the chemical composition of cell walls of raw and cooked ‘Scarlet Warren’ squash. The paper also describes the application of solid-state <sup>13</sup>C NMR to study the molecular motion of the polysaccharides in the squash cell walls.

## MATERIALS AND METHODS

**Plant Material.** ‘Scarlet Warren’ squash was grown during the summer–autumn season on a farm associated with the New Zealand Institute for Crop and Food Research Limited at Kimberley Road, Levin, New Zealand (geographical location 40° 39′ S, 175° 16′ E). The squashes were tagged on the first day of flowering and harvested 50 days after flowering. The harvested squashes were washed, dried, and stored for 2 months at 12 °C and 80–85% relative humidity. After storage, six squashes were allowed to warm to room temperature, and each was marked into 10 equal segments. Every alternate segment of each squash, excluding portions of the skin, seeds, and placental bundle tissues, were frozen in liquid nitrogen and stored at –80 °C for the cell wall isolation of raw squash tissue. All of the remaining segments were steamed until edible (approximately 6–10 min) and then immediately

**Table 2.** Polysaccharide Composition of Cell Walls and Second HEPES-Soluble Fraction of Raw and Cooked ‘Scarlet Warren’ Squash after 2 Months of Storage Determined by GC-MS and Expressed as Mole %<sup>a</sup>

polysaccharide	raw cell walls	cooked cell walls	including starch		excluding starch	
			raw second HEPES	cooked second HEPES	raw second HEPES	cooked second HEPES
galacturonan + RG	25.9	26.8	69.5	7.5	79.6	75.1
arabinan	1.0	1.4	1.2	nd	1.4	nd
arabinogalactan	12.5	11.3	16.3	1.9	18.6	19.0
xyloglucan	4.2	4.0	nd	nd	nd	nd
heteroxylan	1.0	1.3	nd	nd	nd	nd
heteromannan	3.1	3.5	tr	nd	tr	nd
$\alpha$ -cellulose	47.4	46.4	nd	nd	nd	nd
starch	nd	nd	12.6	84.7	nd	nd
total (assigned)	95.1	94.7	99.6	94.1	99.6	94.1

<sup>a</sup>Data represent the mean of three analyses. tr, trace (<0.1%); nd, not detected; RG, rhamnogalacturonan.

frozen in liquid nitrogen and stored at  $-80\text{ }^{\circ}\text{C}$  for the cell wall isolation of cooked squash tissues.

**Isolation of Cell Walls.** Cell walls were isolated from raw and cooked tissues of ‘Scarlet Warren’ squash using the method described previously<sup>20,39</sup> with the following modifications. Frozen powder (50 g of fresh weight) was layered with HEPES buffer (pH 6.8) containing dithiothreitol (DTT) (100 mL), allowed to thaw, and stirred to form a thick slurry. The slurry was homogenized (20500 rpm,  $3 \times 20$  s bursts) in an Ultra-Turrax (T25 Basic, INK Labortechnik Works). The suspension was filtered through  $53\text{ }\mu\text{m}$  nylon mesh and washed with cold HEPES–DTT buffer (pH 6.8) (200 mL). The filtrate was designated “first HEPES-soluble fraction”. The residue was ground ( $3 \times 2$  min) in a ring grinder (Rocklab, Auckland, New Zealand). The suspension was washed with cold HEPES–DTT buffer (pH 6.8) (100 mL), filtered through a  $53\text{ }\mu\text{m}$  nylon mesh. The residue was washed with cold HEPES–DTT buffer (pH 6.8) (200 mL). The combined filtrate was designated “second HEPES-soluble fraction”. The residue was suspended in 90% v/v aqueous DMSO (200 mL) solution for 24 h with stirring to gelatinize the starch granules. This was followed by filtration and washing as described above. The residue was resuspended in HEPES buffer (pH 6.8) (100 mL) and incubated with porcine  $\alpha$ -amylase (220 units, type 1-A, Sigma) at  $25\text{ }^{\circ}\text{C}$  for 1 h with stirring. The suspension was filtered through glass microfiber filters to obtain the purified cell walls.

**Carboxyl Reduction.** The esterified uronic acid residues in the cell walls were reduced with  $\text{NaBD}_4$ .<sup>40</sup> Free uronic acid residues were subsequently derivatized with 1-cyclo-3-(2-morpholinoethyl)carbodiimide metho-*p*-toluenesulfonate and reduced either with  $\text{NaBD}_4$  to determine total uronic acids or with  $\text{NaBH}_4$  to determine the degree of esterification of the uronic acid, respectively.<sup>41</sup>

**Linkage Analysis of Polysaccharides.** The carboxyl-reduced samples were methylated using  $\text{NaOH}/\text{CH}_3\text{I}$ <sup>42</sup> as modified by Nunan et al.<sup>40</sup> Hydrolysis and reduction were performed according to the method of Harris et al.<sup>43</sup> Each linkage analysis was done in triplicate.

**Solid-State  $^{13}\text{C}$  Nuclear Magnetic Resonance Spectroscopy.** Cell wall samples were air-dried to water contents of 59, 51, 37, and 28% for raw and 76, 66, 60, 47, 36, 28, and 12% for cooked samples. Water contents were determined by recording the mass of the sample at each stage of partial drying and then fully drying the sample when all of the NMR experiments were completed. Each sample was packed in a 7 mm diameter cylindrical silicon nitride ( $\text{Si}_3\text{N}_4$ ) NMR rotor, retained with Vespel end-caps, and spun at 4 kHz in a Doty Scientific magic-angle spinning (MAS) probe for  $^{13}\text{C}$  CP/MAS NMR spectroscopy at 50.3 MHz on a Varian Inova-200 spectrometer. Single-pulse excitation (SPE/MAS) NMR spectra were obtained with a  $6\text{ }\mu\text{s}$ ,  $90^{\circ}$   $^{13}\text{C}$  pulse followed by 51 ms of data acquisition and a 1 s recovery delay.

The PSRE experiments required acquisition of two spectra, labeled S and S'. The normal CP/MAS NMR spectrum (S) was obtained with a  $5.5\text{ }\mu\text{s}$  proton preparation pulse, a 1 ms cross-polarization contact time, 51 ms of data acquisition, and a 1 s recovery delay, to allow  $T_1(\text{H})$  relaxation. This sequence was repeated at least 17000 times to improve the signal-to-noise ratio. The partly relaxed spectrum (S') was acquired with the same pulse sequence, except for a 4 ms proton spin-locking pulse inserted between the proton preparation pulse and the contact time, so that the signal strengths were affected by  $T_{1\rho}(\text{H})$  relaxation. The proton decoupling field strength was 49–62 kHz for all samples. Chemical shifts are reported relative to tetramethylsilane (TMS).

The PSRE NMR subspectra were generated by exploiting differences in the relaxation time constant  $T_{1\rho}(\text{H})$  between different domains. The PSRE procedure has been described in detail.<sup>31,44,45</sup> The sample contains two types of domains, labeled A and B, which are associated with rigid and mobile components, respectively. The signal at 89 ppm, assigned to the crystallite interior of cellulose, was selected as characteristic of subspectrum A and was therefore eliminated from subspectrum B. A shoulder at 69 ppm, assigned to noncellulosic polysaccharides (primarily pectin), was selected as characteristic of subspectrum B and eliminated from subspectrum A. The linear combinations used to obtain the PSRE subspectra for raw squash cell walls were  $-0.8\text{S} + 2.9\text{S}'$  for subspectrum A and  $1.8\text{S} - 2.9\text{S}'$  for subspectrum B, and those for cooked squash cell walls were  $-1.5\text{S} + 3.3\text{S}'$  for subspectrum A and  $2.5\text{S} - 3.3\text{S}'$  for subspectrum B.

## RESULTS AND DISCUSSION

No difference was found in the yield of cell walls isolated from raw squash ( $13.9 \pm 0.8\text{ mg/g}$ ) and that of cooked squash ( $14.1 \pm 1.0\text{ mg/g}$ ).

**Linkage Analysis of Cell Wall Polysaccharides.** The cell walls of raw and cooked squash showed no major differences in either the linkage analyses (Table 1) or the polysaccharide compositions (Table 2). The most abundant linkage type observed in ‘Scarlet Warren’ squash cell walls was 4-linked glucopyranose (4-Glcp) (Table 1), which is the sole linkage in cellulose but also occurs in xyloglucan and glucomannans.

The second most abundant glycosyl linkage in squash cell walls was a 4-linked galacturonic acid (4-GalAp) residue. The 4-GalAp content (combined, free; 4-GalAp and methyl esterified; 4-GalApOMe) of both raw and cooked squash was 24 mol % of the total composition of respective cell walls (Table 1). The degrees of esterification of 4-GalAp residues for raw and cooked tissues were similar (71 and 76 mol %, respectively).

Pitchkina et al.<sup>26</sup> reported the degree of esterification of pumpkin pectin as 65%.

The 4-linked galactopyranosyl (4-Galp) residue accounted for 11 and 10 mol % of the total composition of raw and cooked cell walls, respectively (Table 1). All other linkage types each represent  $\leq 3.5$  mol % of the carbohydrate composition of the cell walls. The linkage analysis results are consistent with the monosaccharide composition of the polysaccharides sequentially extracted from 'Scarlet Warren' squash cell walls.<sup>22</sup>

The second HEPES-soluble fraction was selected for linkage analysis because this fraction extracted the water-soluble pectic polysaccharides and it contained fewer cytoplasmic contaminants than the first HEPES-soluble fraction. The yields of the first HEPES-soluble fraction were 10 and 9% (by dry weight) of the cell wall for raw and cooked squash, respectively. The yield of the second HEPES-soluble fraction isolated from both the raw and cooked squash was 5% (by dry weight) of the cell wall. The 4-Glcp in the second HEPES-soluble fraction, primarily derived from starch, accounted for 13 mol % total composition of the fraction in raw squash, whereas in cooked squash it accounted for 78 mol % of the total composition of the fraction (Table 1). The predominant glycosyl linkage in the second HEPES-soluble fraction of raw tissues of squash was 4-GalAp residues (combined; 4-GalAp and 4-GalApOMe), accounting for 68 mol % the total composition of the fraction. In contrast, the amount of total 4-GalAp (combined 4-GalAp and 4-GalApOMe) in this fraction from cooked tissues of squash was 49 mol %, excluding starch.

The degrees of esterification of 4-GalAp residues extracted from the second HEPES-soluble fraction of raw and cooked squash were 63 and 57 mol %, respectively. The decrease in the degree of esterification of the second HEPES-soluble fraction after cooking could be due to greater water solubility of less esterified pectins with the more esterified pectins remaining in the cell walls (76 mol % for cooked versus 71 mol % for raw).

The polysaccharide compositions of the cell walls and the second HEPES-soluble fraction of raw and cooked 'Scarlet Warren' (Table 2) were calculated from the totals of individual glycosyl residues, which are characteristic of cell wall polysaccharides.<sup>9,40,46</sup> The xyloglucan content was estimated from the sum of 4,6-Glcp, 4-Glcp equivalent to one-third of 4,6-Glcp, terminal and 2-linked xylopyranose (2-Xylp), terminal Galp equivalent to 2-Xylp, and terminal fucopyranose (t-Fucp). The remaining 4-Glcp was assumed to be cellulose. Xylan was estimated from 4-Xylp, 2,4-Xylp, and 3,4-Xylp. Arabinan would be estimated from 5-linked arabinofuranose (5-Araf) and 3,5-Araf and terminal Araf equivalent to the value of 3,5-Araf. However, the amount of 3,5-Araf was unable to be quantified in this work because 3,5-Araf was eluted at the same time as 4-Galp. Hence, arabinan is estimated from 5-Araf only and is thus underestimated. Galacturonan (both rhamnogalacturonan and homogalacturonan) was estimated from the sum of 4-GalAp, 4-GalApOMe ester, 2-Rhap, and 2,4-Rhap. Galactan was estimated from the sum of 4-Galp, 4,6-Galp, and terminal Galp equivalent to 4,6-Galp. Mannan was estimated from 4-Manp, 4,6-Manp, and terminal 4-Galp equivalent to 4,6-Galp. The starch content in the second HEPES-soluble fraction was estimated from the sum of 4-Glcp, 4,6-Glcp, and terminal Glcp equivalent to 4,6-Glcp.

It is noteworthy that cellulose was the principal component amounting to 46–47 mol % of total cell wall polysaccharide (Table 2). Furthermore, the cell walls of 'Scarlet Warren' squash contain unusually low amounts of xyloglucan (4 mol %) and xylan (1 mol %), although comparable amounts are found

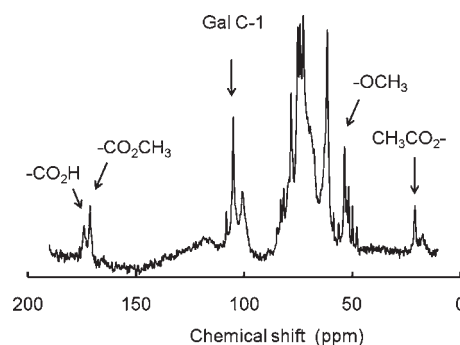


**Figure 1.** SPE  $^{13}\text{C}$  NMR spectrum of raw 'Scarlet Warren' squash cell walls at 59% moisture content.

in celery<sup>9</sup> and sugar beet.<sup>10</sup> The percentages of galacturonan (both rhamnogalacturonan and homogalacturonan) were similar (26–27 mol %) in both raw and cooked cell walls. Total pectic polysaccharide (galacturonan, rhamnogalacturonan, arabinan, and arabinogalactan) content of the cell walls of raw and cooked squash was 39 mol % each of the respective cell walls, calculated by excluding the water-soluble pectic polysaccharides.

The amounts of arabinan, arabinogalactan, xyloglucan, and cellulose present in the squash did not change on cooking, leading to the conclusion that overall the cell wall composition was not altered by heating. This is despite the considerable changes in texture as a result of cooking that have previously been measured.<sup>23</sup> A possible explanation is that cooking reduces the interaction of the cell wall polysaccharides to a moderate extent, but otherwise they are unchanged. In support of this idea we note that while the amount of uronic acid in the cell walls did not change with cooking, the uronic acid-containing polysaccharide soluble in water (combined cooking water and the two HEPES fractions) increased by 11% and in the combined CDTA and 0.1 M  $\text{Na}_2\text{CO}_3$  fractions by 10%.<sup>22,47</sup>

**SPE NMR of Cell Walls of 'Scarlet Warren' Squash.** The SPE  $^{13}\text{C}$  NMR technique is used to elicit responses from the more mobile polysaccharides in the cell wall samples. The SPE spectrum from raw 'Scarlet Warren' squash cell walls at 59% moisture content is shown Figure 1. Pectic polysaccharides are visible in the SPE  $^{13}\text{C}$  NMR spectra presumably because of the gel-like structure ascribed to pectins in the cell walls; hence, they are the most mobile of the cell wall polysaccharides. From the spectra of both raw and cooked samples, a large number of well-defined peaks were assigned to pectic polysaccharides (Table 3). The signals were due primarily to galactose, arabinose, and methoxyl pectic polysaccharides. This was consistent with a mobile domain, which cannot be probed using CP/MAS  $^{13}\text{C}$  NMR studies. The most dominant of the sharp signals can be assigned to galactan composed of (1 $\rightarrow$ 4)-linked  $\beta$ -D-galactopyranosyl residues (Figure 1; Table 3). The peak at 61.6 ppm is assigned to C6 of galactose, whereas the signal at 105.1 ppm is assigned to C1 and that at 78.4 ppm is assigned to C4. The presence of galactan in the SPE  $^{13}\text{C}$  NMR spectra of squash cell walls was consistent with the results of the linkage analysis, which revealed relatively large amounts of 4-linked galactopyranosyl residues (Table 1).

Galacturonans are linear chains of  $\alpha$ -(1 $\rightarrow$ 4)-linked galacturonic acid, which may be free acids or substituted by methyl esterification or by acetylation at carbon 2 and/or 3. The signal due to the C-6 carboxyl carbon of polygalacturonic acid is shifted from 175 to 171 ppm when free acid becomes methyl esterified.

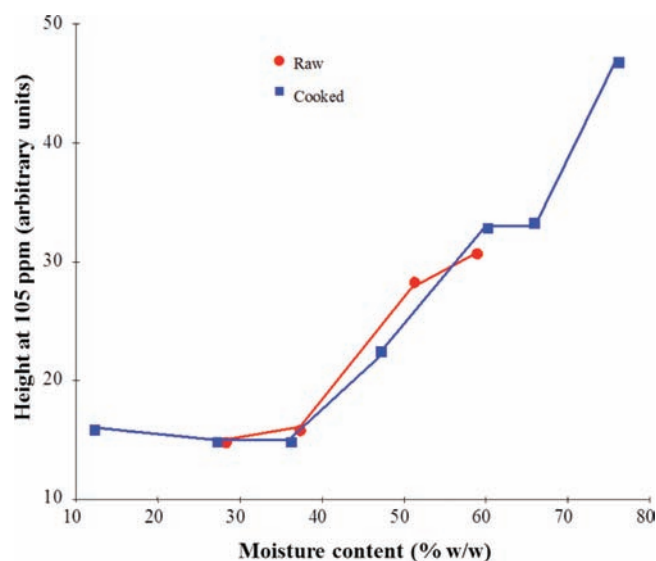
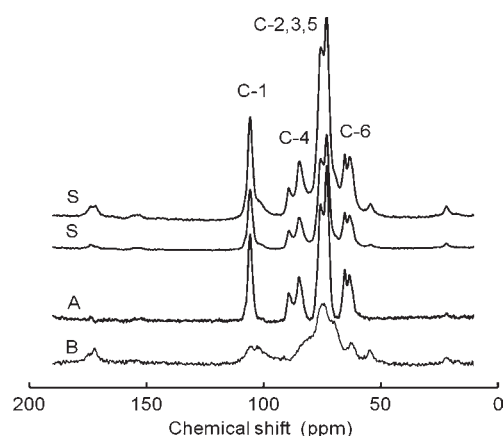


**Table 3.** Chemical Shifts for Polygalacturonic Acid, Galactan, and Arabinan Peaks in SPE  $^{13}\text{C}$  NMR Spectra of ‘Scarlet Warren’ Squash Cell Walls<sup>a</sup>

polysaccharide	carbon atom	literature value	assigned peak
galacturonic acid	1	101.0	101.0
	2	68.7	68.8
	3	69.7	69.5
	4	78.6	79.4
	5	72.1	c
	6	175.0	174.0
esterified galacturonic acid	6	171.1	171.5
	7	53.4	53.7
acetylated galacturonic acid	8	173.0	173.0
	9	21.3	21.2
galactan (1,4)-galactose	1	105.2	105.1
	2	72.8	72.9
	3	74.2	74.2
	4	78.5	78.4
	5	75.4	75.4
	6	61.7	61.6
t-arabinofuranose	1	108.0	108.3*
	2	82.5	81.3
	3	77.8	77.8*
	4	85.2	84.8
	5	62.3	62.9
(1,5)-arabinofuranose	1	108.2	108.3*
	2	82.2	82.3*
	3	77.8	77.8*
	4	83.4	83.1*
	5	67.4	67.9*
3-substituted (1,5)-arabinofuranose	1	108.2	108.3*
	2	81.4	c
	3	84.3	c
	4	82.5	82.3*
	5	67.7	67.9*
2-substituted (1,5)-arabinofuranose	1	107.6	u
	2	88.2	u
	3	76.4	s
	4	83.4	83.1*
	5	67.7	67.9*

<sup>a</sup> Peaks were assigned using literature values.<sup>9,29,32,34,48–50</sup> When the absorptions of two different carbon atoms correspond to form a common peak, they are labeled with an asterisk (\*). A peak that is indistinct or completely covered by another is labeled “c”, and a peak that is visible as a shoulder on the side of other peak is labeled “s”. An unassigned peak is labeled “u”.

The peak at 53.7 ppm is assigned to the methyl ester carbon, whereas the peak at 21.2 ppm is assigned to the acetyl carbon

**Figure 2.** Height of the signal at 105 ppm (C-1 of galactosyl residues) versus moisture content for SPE  $^{13}\text{C}$  NMR experiments on cell wall polysaccharides from raw and cooked ‘Scarlet Warren’ squash.**Figure 3.** CP/MAS  $^{13}\text{C}$  NMR spectra of raw ‘Scarlet Warren’ squash cell walls over the range 10–190 ppm: S was obtained by the normal pulse sequence, and S’ was obtained with an additional 4 ms of proton spin-locking pulse. PSRE subspectra A and B are generated from S and S’, and the signals are primarily for the cellulose and noncellulosic matrix respectively.

(Table 3). The methoxyl carbon signals at 53.7 ppm in both raw and cooked (not shown) squash were clearly distinguished and were apparently unaffected by cooking, which might be expected from their similar degrees of esterification (71 and 76%, respectively; Table 1). The relative heights of the signals at 171 and 174 ppm confirmed the high levels of esterification (Figure 1). The peak assignments for arabinan and arabinogalactan are given in Table 3.

SPE NMR spectra at different moisture contents were recorded for the cell walls of raw and cooked tissues. Partial drying of the cell walls was intended to test the moisture content at which the more mobile polysaccharides became immobilized. The SPE spectra from the cell walls having higher moisture contents were more detailed in comparison to those at lower moisture contents. All of the sharp signals seen at higher moisture

**Table 4. Chemical Shift for Crystalline Cellulose Signals Observed by CP/MAS  $^{13}\text{C}$  NMR Compared with Literature Values<sup>9,29,32,38 a</sup>**

carbon atom	chemical shift (ppm from TMS)	
	literature value (i, s)	assigned peak (i, s)
1	105.5	105.3
2	73.0, 75.0	72.7, 75.5
3	73.0, 75.0	72.7, 75.5
4	84.9, 89.4	84.4, 89.0
5	73.0, 75.0	72.7, 75.5
6	62.5, 65.4	62.8, 65.0

<sup>a</sup> “i” denotes peaks due to cellulose chains in the crystallite interior, and “s” denotes peaks due to cellulose on the crystallite surface.

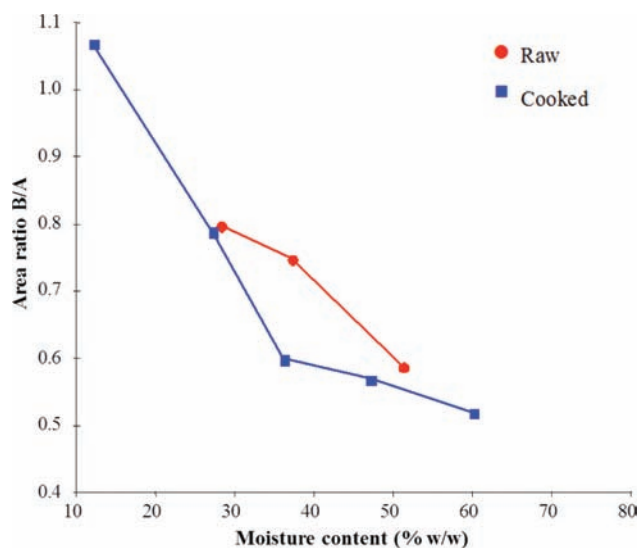


**Figure 4.** Plot of the ratio of signal areas of subspectra B and A versus moisture content for cell wall polysaccharides from raw and cooked ‘Scarlet Warren’ squash.

contents broadened as the samples were dried to lower moisture contents. Tang et al.<sup>30</sup> reported a similar marked increase in signal intensities of galactan and galacturonan in the SPE  $^{13}\text{C}$  NMR spectra with higher moisture contents. The height at signal 105 ppm (C-1 of galactosyl residue) versus moisture content (Figure 2) shows the effect of the water content on the molecular mobility of the galactan. The galactans in both raw and cooked squash become immobilized at below 40% moisture. The similar plots obtained for raw and cooked squash suggest that cooking had no effect on the highly mobile galactan portion of the cell wall.

**Assignment of Signals in PSRE NMR Spectra.** The PSRE NMR subspectra were generated by exploiting differences in the relaxation time constant  $T_{1\rho}(\text{H})$  between different domains. The normal  $^{13}\text{C}$  NMR spectrum of raw squash cell walls (S in Figure 3) is dominated by signals assigned to cellulose. The assignment of cellulose is based on the published chemical shifts values (Table 4). Weaker signals at 22 ppm are assigned to the acetyl groups. The signals at 54 ppm are assigned to the methoxyl carbon, whereas the signals at 171 and 174 ppm are assigned to the carboxylic carbon in methyl esterified and free galacturonic acid, respectively.<sup>28,30,32</sup>

**Table 5. Area Ratio of Subspectra B/A and  $T_{1\rho}(\text{H})$  Values Obtained from PSRE Experiments<sup>a</sup>**

domain type	ratio (B/A)	$T_{1\rho}(\text{H})$ (ms)
raw	0.71 ± 0.11	
A		9.0 ± 0.1
B		3.7 ± 0.1
cooked	0.65 ± 0.12	
A		10.0 ± 0.1
B		4.1 ± 0.9

<sup>a</sup> Values are expressed as the mean ± SD of three values computed from the PSRE experiments at three different moisture contents, 51, 37, and 28% for raw and 47, 36, and 28% for cooked ‘Scarlet Warren’ squash cell walls.

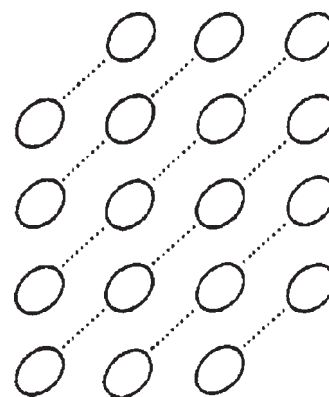


**Figure 5.** Theoretical model of a possible cross section through a cellulose microfibril crystallite with 33% crystal interior cellulose.

The subspectra A from raw and cooked ‘Scarlet Warren’ cell walls show signals that can be assigned to cellulose (Table 4), and the signals in the subspectra B can be assigned to pectic polysaccharides (Table 3 and previous discussion). The ratio of the signal areas B/A increased for each sample with decreasing water content (Figure 4), as expected for a constant response from subspectra A but increasingly solid-like molecular dynamics in subspectra B (drying the samples made the pectic polysaccharides less mobile, so they contributed stronger signals to subspectra B). If the pectic polysaccharides became more mobile due to cooking, they would contribute less to the semimobile material monitored by subspectrum B and the signal area ratio B/A would decrease compared to the raw sample. This was observed only at about 37% moisture content for cooked squash cell walls, which had a slightly lower area ratio B/A than that for raw squash, suggesting that cooking caused a decrease in the rigidity of a small portion of pectic polysaccharides. The small increase in water-soluble pectic polysaccharides on cooking<sup>22</sup> supports this interpretation. However, the mean area ratios B/A (Table 5) for three different moisture contents are similar for raw and cooked cell walls. Therefore, overall cooking caused little or no change in the mobility of pectic polysaccharides.

The ratios of the heights of relevant peaks in spectra S and S' were used to calculate the spin relaxation time constant  $T_{1\rho}(\text{H})$ . The values of  $T_{1\rho}(\text{H})$  (Table 5) are the mean of three values computed from the PSRE experiments at three different moisture contents for raw and cooked cell walls. The editing procedures based on  $T_{1\rho}(\text{H})$  can probe domains of dimensions 2–30 nm.<sup>51</sup> The greater the

separation between cellulose and noncellulosic polysaccharides, the greater the difference between  $T_{1\rho}(H)$  for subspectra A and B. Very long  $T_{1\rho}(H)$  values for subspectrum A are regarded as the intrinsic value for cellulose, whereas relatively shorter  $T_{1\rho}(H)$  values would indicate a close association of cellulose with noncellulosic polysaccharides. The  $T_{1\rho}(H)$  values (Table S) from subspectrum A for raw and cooked squash cell walls were similar, indicating cooking produced no detectable change. A comparable value of 9.7 ms was observed for raw apple cell walls.<sup>28</sup> The  $T_{1\rho}(H)$  values for subspectra B were indistinguishable, also suggesting cooking produced no change.

**Cross-Sectional Dimensions of Cellulose Crystallite.** The subspectra A from the crystalline cellulose showed the C-4 signal split into two peaks at 89 and 84 ppm, which are assigned to crystallite interior and crystallite surface cellulose, respectively. Relative areas of the C-4 signals in subspectrum A were used to determine a parameter  $X$ , interpreted as the fraction of cellulose chains contained within crystallite interiors.<sup>28,35</sup> Parameter  $X$  was calculated by using the signal areas measured between vertical lines drawn at 80, 87, and 93 ppm on the expanded C-4 region of subspectrum A. The value of  $X$  was  $0.33 \pm 0.01$  for raw and  $0.34 \pm 0.02$  for cooked squash. Hence, cooking did not alter the proportion of interior to surface cellulose chains in the crystalline microfibrils.

From the relative proportions of cellulose crystallite interior and crystallite surface chains, it is possible to draw a model structure for the squash cellulose in a  $5 \times 4$  array (Figure 5). This model has 6 chains (33.3%) in the interior, each hydrogen bonded to 2 adjacent chains, and 12 chains (66.6%) on the surface, with each hydrogen-bonded to 1 adjacent chain. The model has cross-sectional dimensions of  $\sim 3$  nm, which is typical of cellulose microfibrils in parenchyma cell walls.<sup>9,28,33,38</sup>

Overall, little or no change in the mobility/rigidity of the cell wall polysaccharides was detected as a result of cooking the squash. Hence, the changes of texture we measured on cooking<sup>23</sup> may be attributed to other causes. Rheological measurements are on a macroscopic scale, whereas solid-state NMR works at the nanometer scale level. Consequently, the softening of texture detected on cooking may be due to reduced adhesion of adjacent cells, whereas the walls of the cells are largely unaltered. A change in turgor pressure and swelling of the starch granules could also be involved.

## AUTHOR INFORMATION

### Corresponding Author

\*E-mail: l.melton@auckland.ac.nz. Phone: 649-3737599. Fax: 649-3737422.

### Present Addresses

<sup>†</sup>Scion, Rotorua, New Zealand.

### Funding Sources

We thank the New Zealand Plant and Food Research Institute (formerly New Zealand Institute for Crop and Food Research) for financial assistance.

## ACKNOWLEDGMENT

We thank the New Zealand Plant and Food Research Institute (formerly New Zealand Institute for Crop & Food Research) for squash samples. We also thank Paul L. Hurst for useful discussions and initiating the project.

## REFERENCES

- (1) Thompson, D. S. Space and time in the plant cell wall: relationships between cell type, cell wall rheology and cell function. *Ann. Bot.* **2008**, *101*, 203–211.
- (2) Martin, C.; Bhatt, K.; Baumann, K. Shaping in plant cells. *Curr. Opin. Plant Biol.* **2001**, *4*, 540–549.
- (3) Labavitch, J. M. Cell wall turnover in plant development. *Plant Physiol.* **1981**, *31*, 385–406.
- (4) Davies, L. M.; Harris, P. J. Atomic force microscopy of microfibrils in primary cell walls. *Planta* **2003**, *217*, 283–289.
- (5) Satiat-Jeunemaitre, B.; Martin, B.; Hawes, C. Plant cell wall architecture is revealed by rapid-freezing and deep-etching. *Protoplasma* **1992**, *167*, 33–42.
- (6) Thimm, J. C.; Burritt, D. J.; Ducker, W. A.; Melton, L. D. Celery (*Apium graveolens* L.) parenchyma cell walls examined by atomic force microscopy: Effect of dehydration on cellulose microfibrils. *Planta* **2000**, *212*, 25–32.
- (7) Marga, F.; Grandbois, M.; Cosgrove, D. J.; Baskin, T. I. Cell wall extension results in the coordinate separation of parallel microfibrils: evidence from scanning electron microscopy and atomic force microscopy. *Plant J.* **2005**, *43*, 181–190.
- (8) Thimm, J. C.; Burritt, D. J.; Ducker, W. A.; Melton, L. D. Pectins influence microfibril aggregation in celery cell walls: an atomic force microscopy study. *J. Struct. Biol.* **2009**, *168*, 337–344.
- (9) Thimm, J. C.; Burritt, D. J.; Sims, I. M.; Newman, R. H.; Ducker, W. A.; Melton, L. D. Celery (*Apium graveolens*) parenchyma cell walls: cell walls with minimal xyloglucans. *Physiol. Plant.* **2002**, *116*, 164–171.
- (10) Renard, C. M. G. C.; Thibault, J.-F. Structure and properties of apple and sugar-beet pectins extracted by chelating agents. *Carbohydr. Res.* **1993**, *244*, 99–114.
- (11) Bootten, T. J.; Harris, P. J.; Melton, L. D.; Newman, R. H. Solid-state <sup>13</sup>C-NMR spectroscopy shows that the xyloglucans in the primary cell walls of mung bean (*Vigna radiata* L.) occur in different domains: a new model for xyloglucan-cellulose interactions in the cell wall. *J. Exp. Bot.* **2004**, *55*, 571–583.
- (12) Zykwiniska, A.; Thibault, J.-F.; Ralet, M.-C. Organization of pectic arabinan and galactan side chains in association with cellulose microfibrils in primary cell walls and related models envisaged. *J. Exp. Bot.* **2007**, *58*, 1795–1802.
- (13) Zykwiniska, A.; Thibault, J.-F.; Ralet, M.-C. Competitive binding of pectin and xyloglucan with primary cell wall cellulose. *Carbohydr. Polym.* **2008**, *74*, 957–961.
- (14) Johnson, K. L.; Jones, B. J.; Schultz, C. J.; Bacic, A. Non-enzymic cell wall glycoproteins. In *The Plant Cell Wall*; Rose, J. K. C., Ed.; Blackwell: Oxford, U.K., 2003; pp 111–154.
- (15) Talbot, L. D.; Ray, P. M. Molecular size and separability features of pea wall polysaccharides. Implications for models of primary cell wall structure. *Plant Physiol.* **1992**, *98*, 357–368.
- (16) Cosgrove, D. J. Wall structure and wall loosening. A look backwards and forwards. *Plant Physiol.* **2001**, *125*, 131–134.
- (17) Ng, A.; Waldron, K. W. Effect of steaming on cell wall chemistry of potatoes (*Solanum tuberosum* cv. Bintje) in relation to firmness. *J. Agric. Food Chem.* **1997**, *45*, 3411–3418.
- (18) Van Marle, J. T.; Stolle-Smits, T.; Donkers, J.; van Dijk, C.; Voragen, A. G. J.; Recourt, K. Chemical and microscopic characterization of potato (*Solanum tuberosum* L.) cell walls during cooling. *J. Agric. Food Chem.* **1997**, *45*, 50–58.
- (19) Ng, A.; Waldron, K. W. Effect of cooking and pre-cooking on cell-wall chemistry in relation to firmness of carrot tissues. *J. Agric. Food Chem.* **1997**, *73*, 503–512.
- (20) Ratnayake, R. M. S.; Hurst, P. L.; Melton, L. D. Texture and the cell wall polysaccharides of buttercup squash 'Delica' (*Cucurbita maxima*). *N. Z. J. Crop Hortic. Sci.* **1999**, *27*, 133–143.
- (21) Quach, M. L.; Melton, L. D.; Harris, P. J.; Burdon, J. N.; Smith, B. G. Cell wall composition of raw and cooked corms of taro (*Colocasia esculenta*). *J. Sci. Food Agric.* **2001**, *81*, 311–318.

- (22) Ratnayake, R. M. S.; Melton, L. D.; Hurst, P. L. Influence of cultivar, cooking, and storage on cell-wall polysaccharide composition of winter squash (*Cucurbita maxima*). *J. Agric. Food Chem.* **2003**, *51*, 1904–1913.
- (23) Ratnayake, R. M. S.; Hurst, P. L.; Melton, L. D. Influence of cultivar, storage and cooking on the mechanical properties of winter squash (*Cucurbita maxima*). *J. Sci. Food Agric.* **2004**, *84*, 433–440.
- (24) Hurst, P. L.; Corrigan, V. K.; Koolaard, J. P. Genetic analysis of sweetness and textural attributes in winter squash (*Cucurbita maxima*). *N. Z. J. Crop Hort. Sci.* **2006**, *34*, 359–367.
- (25) O'Donoghue, E. M.; Somerfield, S. D. Biochemical and rheological properties of gelling isolates from buttercup squash fruit. *Food Hydrocolloids* **2008**, *22*, 1326–1336.
- (26) Ptitchkina, N. M.; Danilova, I. A.; Doxastakis, G.; Kasapis, S.; Morris, E. R. Pumpkin pectin: gel formation at unusually low concentration. *Carbohydr. Polym.* **1994**, *23*, 265–273.
- (27) Evageliou, V.; Ptitchkina, N. M.; Morris, E. R. Solution viscosity and structural modification of pumpkin biopectin. *Food Hydrocolloids* **2005**, *19*, 1032–1036.
- (28) Newman, R. H.; Ha, M. A.; Melton, L. D.  $^{13}\text{C}$  NMR investigation of molecular ordering in the cellulose of apple cell walls. *J. Agric. Food Chem.* **1994**, *42*, 1402–1406.
- (29) Foster, T. J.; Ablett, S.; McCann, M. C.; Gidley, M. J. Mobility resolved  $^{13}\text{C}$ -NMR spectroscopy of primary plant cell walls. *Biopolymers* **1996**, *39*, 51–66.
- (30) Tang, H.; Belton, P. S.; Ng, A.; Ryden, P.  $^{13}\text{C}$  MAS NMR studies of the effects of hydration on the cell walls of potatoes and Chinese water chestnut. *J. Agric. Food Chem.* **1999**, *47*, 510–517.
- (31) Tang, H. R.; Wang, Y. L.; Belton, P. S.  $^{13}\text{C}$  CPMAS studies of plant cell wall materials and model system using proton relaxation-induced spectral editing techniques. *Solid State Nucl. Magn. Reson.* **2000**, *15*, 239–248.
- (32) Jarvis, M. C.; Apperley, D. C. Direct observation of cell wall structure in living plant tissues by solid-state  $^{13}\text{C}$  NMR spectroscopy. *Plant Physiol.* **1990**, *92*, 61–65.
- (33) Newman, R. H.; Davies, L. M.; Harris, P. J. Solid-state  $^{13}\text{C}$  nuclear magnetic resonance characterisation of cellulose in the cell walls of *Arabidopsis thaliana* leaves. *Plant Physiol.* **1996**, *111*, 475–485.
- (34) Smith, B. G.; Harris, P. J.; Melton, L. D.; Newman, R. H. The range of mobility of the non-cellulosic polysaccharides is similar in primary cell walls with different polysaccharides compositions. *Physiol. Plant.* **1998**, *103*, 233–246.
- (35) Newman, R. H. Estimation of the lateral dimensions of cellulose crystallites using  $^{13}\text{C}$  NMR signal strengths. *Solid State Nucl. Magn. Reson.* **1999**, *15*, 21–29.
- (36) Koh, T. H.; Melton, L. D.; Newman, R. H.  $^{13}\text{C}$  NMR characterisation of cell walls of ripening strawberries. *Can. J. Bot.* **1997**, *75*, 1957–1964.
- (37) Ha, M. A.; Apperley, D. C.; Jarvis, M. C. Molecular rigidity in dry and hydrated onion cell walls. *Plant Physiol.* **1997**, *115*, 593–598.
- (38) Smith, B. G.; Harris, P. J.; Melton, L. D.; Newman, R. H. Crystalline cellulose in hydrated primary cell walls of three monocotyledons and one dicotyledon. *Plant Cell Physiol.* **1998**, *34*, 711–720.
- (39) Melton, L. D.; Smith, B. G. Isolation of plant cell walls and fractionation of cell wall polysaccharides. In *Handbook of Food Analytical Chemistry: Water, Proteins, Enzymes, Lipids and Carbohydrates*; Wrolstad, R. E., Ed.; Wiley: Hoboken, NJ, 2005; pp 697–719.
- (40) Nunan, K. J.; Sims, I. M.; Bacic, A.; Robinson, S. P.; Fincher, G. B. Isolation and characterisation of cell walls from mesocarp of mature grape berries (*Vitis vinifera*). *Planta* **1997**, *203*, 93–100.
- (41) Sims, I. M.; Bacic, A. Extracellular polysaccharides from suspension cultures of *Nicotina plumbaginifolia*. *Phytochemistry* **1995**, *38*, 1397–1405.
- (42) Ciucanu, I.; Kerek, F. A simple and rapid method for the permethylation of carbohydrates. *Carbohydr. Res.* **1984**, *131*, 209–217.
- (43) Harris, P. J.; Henry, R. J.; Blakeney, A. B.; Stone, B. A. An improved procedure for the methylation analysis of oligosaccharides and polysaccharides. *Carbohydr. Res.* **1984**, *127*, 59–73.
- (44) Newman, R. H.; Condrón, L. M. Separating subspectra from cross polarisation magic-angle spinning nuclear magnetic resonance spectra by proton spin relaxation editing. *Solid State Nucl. Magn. Reson.* **1995**, *4*, 259–266.
- (45) Newman, R. H. Editing the information in solid-state carbon-13 NMR spectra of food. In *Advances in Magnetic Resonance in Food Science*; Belton, P. S., Hills, B. P., Webb, G. A., Eds.; Royal Society of Chemistry: Cambridge, U.K., 1999; pp 144–157.
- (46) Nunan, K. J.; Sims, I. M.; Bacic, A.; Robinson, S. P.; Fincher, G. B. Changes in cell wall composition during ripening of grape berries. *Plant Physiol.* **1998**, *118*, 783–792.
- (47) Ratnayake, R. M. S. Physicochemical properties of squash (*Cucurbita maxima*) cell walls. Ph.D. thesis, Chemistry Department, University of Auckland, New Zealand, 2000.
- (48) Capek, P.; Toman, R.; Kardosova, A.; Rosik, J. Polysaccharides from the root of marsh mallow (*Althaea officinalis* L.): structure of an arabinan. *Carbohydr. Res.* **1983**, *117*, 133–140.
- (49) Ryden, P.; Colquhoun, I. J.; Selvendran, R. R. Investigation of structural features of the pectic polysaccharides of onion by  $^{13}\text{C}$  NMR spectroscopy. *Carbohydr. Res.* **1989**, *185*, 233–237.
- (50) Jarvis, M. C.; Apperley, D. C. Chain conformation in concentrated pectic gels: evidence from  $^{13}\text{C}$  NMR. *Carbohydr. Res.* **1995**, *275*, 131–145.
- (51) Zumbulyadis, N. Selected carbon excitation and the detection of spatial heterogeneity in cross polarisation magic-angle spinning NMR. *J. Nucl. Magn. Reson.* **1983**, *53*, 486–494.